Chapter 12

Electrodeposition of Zn, Cu, and Zn-Cu Alloys from Deep Eutectic Solvents

Xingli Zou, Xionggang Lu and Xueliang Xie

Additional information is available at the end of the chapter

http://dx.doi.org/10.5772/65883

Abstract

Deep eutectic solvents (DESs) comprising choline chloride (ChCl) with either urea or ethylene glycol (EG) have been successfully used as powerful and potential electrolytes for extracting metals from their corresponding metal oxide precursors. In this work, for electrodeposition of Zn and Zn-Cu alloys, ChCl/urea-based DES was employed. Cyclic voltammetry study demonstrates that the reduction of Zn(II) to Zn is a diffusion-controlled quasi-reversible, one-step, two electrons transfer process. Micro-/nanostructured Zn and Zn-Cu alloys films have been electrodeposited directly from their metal oxide precursors in DES, and the Zn and Zn-Cu alloy films exhibit homogeneous morphologies with controlled particle sizes. Besides, the electrodeposition of Cu from CuO in the eutectics based on ChCl with urea and EG has been investigated, respectively. The higher coordinated Cu species in the ChCl/urea-based DES are obviously more difficult to reduce, and higher overpotential is needed to drive the nucleation process compared with the lower coordinated Cu species in the ChCl/EG-based DES. The surface morphology of the Cu electrodeposits is significantly affected by the type of DES and the electrodeposition potentials. Furthermore, the Cu electrodeposits obtained in the ChCl/urea-based DES possess more dense microstructures than those produced in the ChCl/EG-based DES.

Keywords: electrodeposition, deep eutectic solvents, metal oxides, cyclic voltammetry, morphology

1. Introduction

The electrodeposition of Zn, Cu, and Zn-Cu alloys for corrosion-resistant coatings and electrochemical applications such as electrocatalysis and electronic devices has received considerable attention in recent years [1–7]. The electrodeposition of Zn, Cu, and Zn-Cu alloys

is commonly performed in aqueous electrolyte solutions. Traditional Zn plating is mainly carried out in sulfuric acidic aqueous baths [8, 9]. Generally, Zn is extracted from zinc sulfide ore. The ore is mined from the earth's crust and beneficiated by flotation methods that produce zinc sulfide concentrates. The mineral concentrates are oxidized to metal oxides during high temperature roasting and then the metal oxides are leached with sulfuric acid to produce zinc sulfate solution. Finally, the Zn electrodeposits are obtained from the zinc sulfate electrolyte under constant current electrolysis [10, 11]. However, the traditional Zn electrodeposition process is very sensitive to impurities and requires effective purification methods to produce pure Zn [12]. Copper electrodeposition is mostly performed in aqueous solutions, which possess high solubility of copper salts (e.g., $CuCl_2$ and $CuSO_4$) and high electrolyte conductivity. However, the acid- and cyanide-based aqueous electrolytes are corrosive and the inevitable hydrogen evolution reaction commonly occurs during the electrolysis process [13]. Consequently, finding new alternative electrolytes for the electrodeposition of Zn, Cu, and Zn-Cu alloy films at low temperature has become the focus in recent years.

More recently, the direct electrochemical reduction of metal oxides/compounds to metals/alloys in molten salts has been extensively studied because of its low energy consumption and environmental compatibility [14, 15]. This previous innovative work shows that the production of metallic/coating materials directly from their metal oxide precursors in liquid salt is a promising route. Low-temperature electrolytic production of iron film from iron oxide in alkaline solution has been studied in our previous work [16], which showed that metal oxide has the potential to be used as a precursor for the electrodeposition at low temperature; the electrochemical process can be controlled effectively and the electrodeposition process generally exhibits acceptable current efficiency. However, in comparison with aqueous solutions, room temperature ionic liquids (RTILs) have attracted much interest as promising electrolyte candidates for metal electrodeposition due to their remarkable characteristics, such as high thermal and chemical stability, negligible vapor pressure, wide electrochemical windows, high ionic conductivity, simplicity of handing, and good solubility for quite a lot of metal salts [17–19]. The hydrogen embrittlement and hydrogen evolution reactions occurring in aqueous solutions can be avoided by using ionic liquids as electrolytes. The electrodeposition of Zn has been investigated in many ionic liquids, particularly in $AlCl_3$-based ionic liquids [20] and chlorozincate ionic liquids [21]. In addition, the electrodeposition of Zn from $ZnCl_2$ precursor has also been studied in choline chloride (ChCl)-based deep eutectic solvents (DESs) [22–26]. Liu et al. [27] illustrated the electrodeposition of Zn films from zinc triflate ($Zn(TfO)_2$) in 1-butyl-1-methylpyrrolidinium trifluoromethylsulfonate ($[Py_{1,4}]TfO$) and 1-ethyl-3-methylimidazolium trifluoromethylsulfonate ([EMIm]TfO) ionic liquids. Zheng et al. [28] investigated the electrodeposition of Zn films from ZnO in imidazolium chloride/urea ionic liquid, which suggested that ZnO has appreciable solubility in the electrolyte. Besides, the electrochemical behavior of copper species (e.g., CuCl and $CuCl_2$) has been investigated in a range of ionic liquids such as Lewis acidic, basic chloroaluminate ionic liquids, and air-/water-stable ionic liquids based on $[BF_4]^-$, $[N(CN)_2]^-$, and $[Tf_2N]^-$ [29–34]. Although these ionic liquids show many advantages in electrodeposition of Cu, issues such as toxicity, cost, and tedious synthesis procedures may limit their realistic applications [35]. Furthermore, many air-/water-stable ionic liquids are not

ideal electrolyte for copper salts such as nitrates, halides, and sulfates because of their poor solubilities [36]. Chen et al. [37] attempted to introduce the cuprous ions into the ionic liquid by the anodic dissolution of a Cu electrode, however, it is a time-consuming process. Therefore, searching for suitable ionic liquid-metal precursors systems for the electrodeposition of Zn, Cu, and Zn-Cu alloys is extremely needed.

DESs, which are made from quaternary ammonium salts mixed with hydrogen bond donors, such as carboxylic acids, alcohols, and amides, are promising electrolytes for electrodeposition application [38, 39]. The DESs are simple to prepare, relatively stable in air and moisture, many are biodegradable, and are relatively low cost [40–47]. Moreover, the DESs show considerable selective solubilities for many metal oxides, which may provide a new route for preparation of metals from metal oxide precursors in the DESs [48, 49]. In comparison with $ZnCl_2$, CuCl, and $CuCl_2$ precursors [22–26], ZnO, Cu_2O, and CuO have potential to be used directly as new promising precursors for the electrodeposition of Zn, Cu, and Zn-Cu alloys films in DESs without chloridization pretreatment. ChCl/urea-based DES has been used as a potential solvent for Zn recovery from waste oxide residues [50]. Yang and Reddy [41, 42] studied the electrodeposition of Zn and Pb films from their oxide precursors in the ChCl/urea-based DES due to their relatively high solubilities in the DES. Tsuda et al. [43] investigated the electrochemical behavior of Cu_2O in the same DES, and they found that Cu can be directly electrodeposited from Cu_2O precursor. More recently, we have also found that micro-/nanostructured Zn and Cu films can be electrodeposited from ZnO and CuO precursors in DESs, respectively [44, 45]. Zhang et al. [46] also demonstrated that the electrochemical synthesis of uniform Cu nanoparticles from Cu_2O can be achieved in ChCl/urea-based DES. This previous work generally showed that zinc and copper oxides have the potential to be used as the precursors for the direct electrodeposition of Zn, Cu, and Zn-Cu alloys films in DESs.

2. Electrodeposition of Zn from ZnO in ChCl/urea-based DES

2.1. Cyclic voltammetry (CV) analysis

The blank CV curve obtained from a platinum working electrode in ChCl/urea-based DES at 333 K is illustrated in **Figure 1(a)**. The cathodic limit is approximately –1.2 V and the anodic limit is about 1.2 V. It can be seen from the blank CV that the electrochemical window of the ChCl/urea-based DES is approximately 2.4 V. **Figure 1(b)** shows the CV curve obtained from a platinum working electrode in the ChCl/urea-based DES dissolved with 0.1 M ZnO at 333 K and potential range of –1.3 to –0.1 V. As evidenced from this figure, the single cathodic current peak observed at about –1.1 V is attributed to the reduction of Zn^{2+} to the metal Zn, the anodic current peak occurred at approximately –0.95 V and is due to the stripping of the electrodeposited Zn.

In order to further investigate the electrochemical behavior of Zn, CV experiments using a platinum electrode as working electrode at different scan rates in ChCl/urea–ZnO (0.1 M) were also performed systematically, and the CV curves are shown in **Figure 2(a)**.

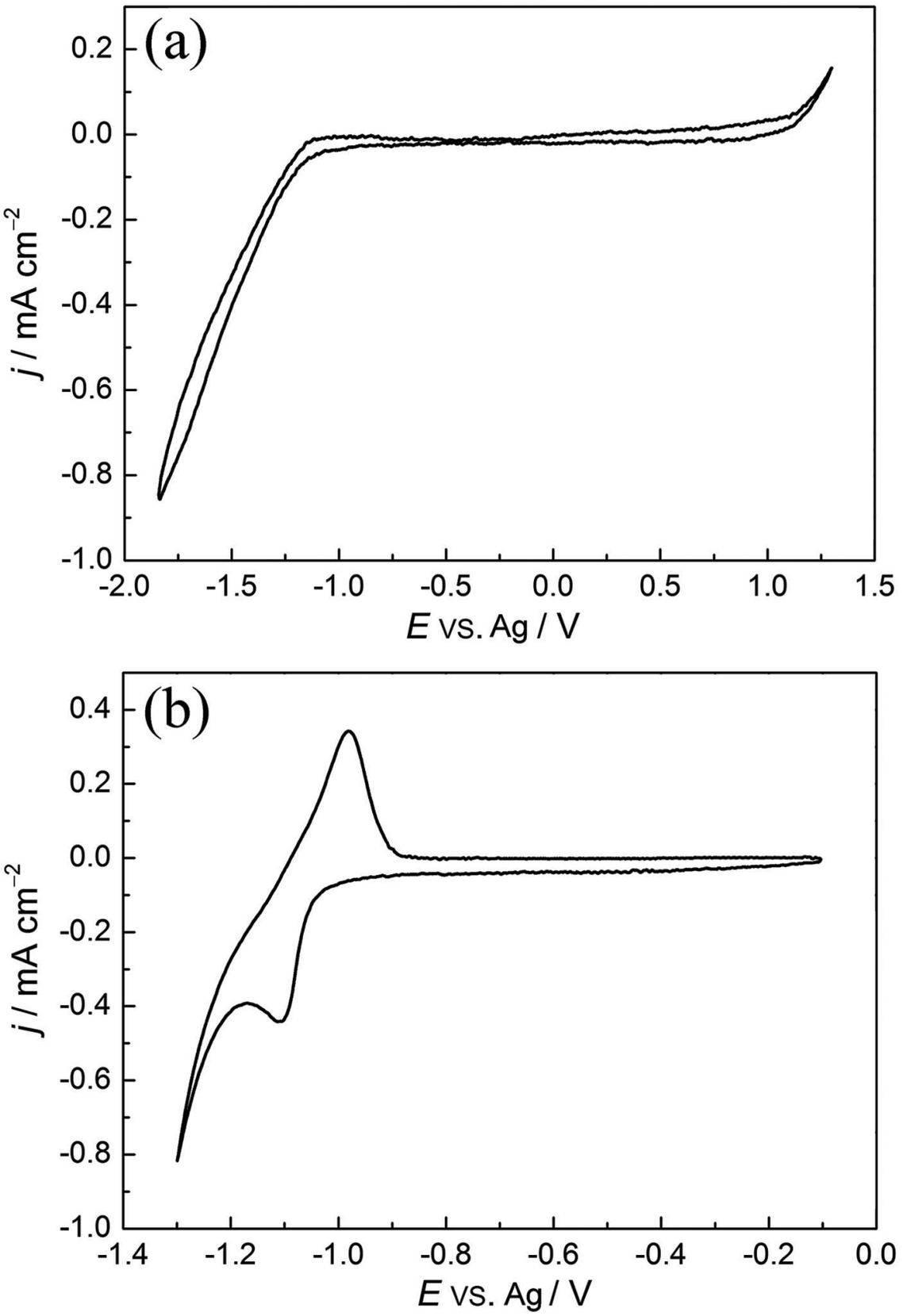

Figure 1. (a) CV curve of a Pt electrode in pure ChCl/urea at 333 K with a scan rate of 10 mV s^{-1}. (b) CV curve of a Pt electrode in ChCl/urea–ZnO (0.1 M) at 333 K with a scan rate of 10 mV s^{-1}.

http://dx.doi.org/10.5772/65883

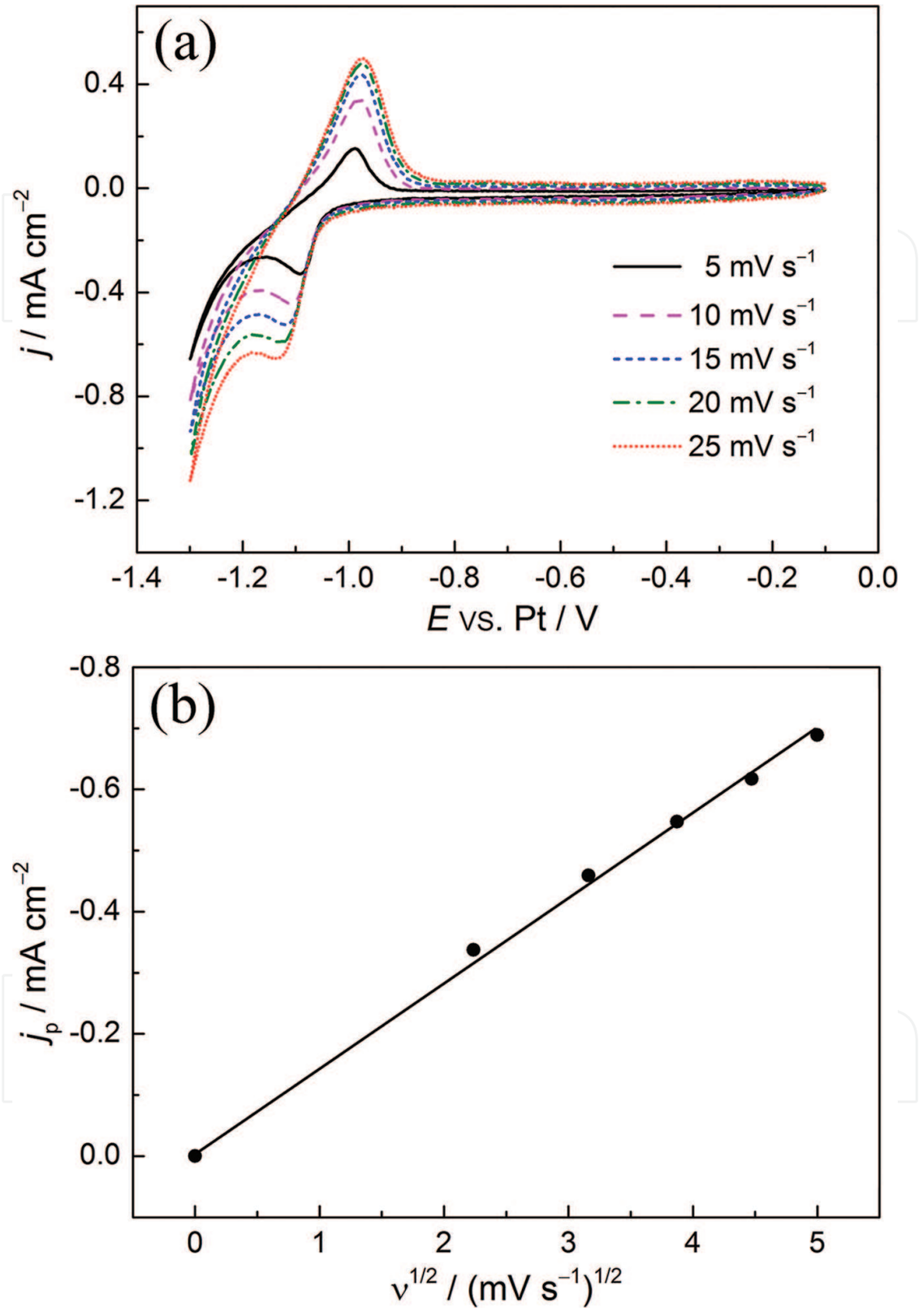

Figure 2. (a) CV curve of a Pt electrode in ChCl/urea–ZnO (0.1 M) at 333 K with different scan rates. The scan rates were 5, 10, 15, 20, and 25 mV s^{-1}, respectively. (b) Relationship between cathodic peak current density (j_{pc}) and square root of scan rate ($\nu^{1/2}$) calculated from (a).

The cathodic and anodic peak's current densities increase with the increase of scan rate, and the cathodic and anodic peak potentials shift to more negative and positive sides, respectively. In **Figure 2(b)**, the cathodic peak current density (j_{pc}) vary linearly as a function of the square root of scan rate ($\nu^{1/2}$), implying the reduction process of Zn(II) is mainly diffusion-controlled. Besides, the cathodic peak and half-peak potentials $|E_{pc} - E_{pc/2}|$ increase with the increase of scan rate. At the lowest scan rate, the difference in the value of 42 mV is larger than the value for the reversible process (31 mV at 333 K). All of these results suggest that the reduction of Zn(II) to Zn in ChCl/urea-based DES is a diffusion-controlled quasi-reversible process [51].

For a quasi-reversible charge transfer process, the diffusion coefficient of Zn(II) can be determined by the irreversible Randles-Sevick equation (1) [51], which is applicable to the quasi-reversible systems as well [52, 53],

$$j_{pc} = 0.4958nFAC_{Zn(II)}D_{Zn(II)}^{1/2}\left(\frac{\alpha n_{\alpha}F\nu}{RT}\right)^{1/2} \tag{1}$$

where j_{pc} is the cathodic peak current density, F is the Faraday constant, n is the number of exchanged electrons, $C_{Zn(II)}$ is the Zn(II) species concentration, A is the electrode area, $D_{Zn(II)}$ is the diffusion coefficient of Zn(II) species, ν is the scan rate, α is the transfer coefficient, n_{α} is the electron transfer number in the rate determining step, R is the gas constant, and T is the absolute temperature. The value α can be obtained from Eq. (2) [51]:

$$\left|E_{pc} - E_{pc/2}\right| = 1.857RT/\alpha n_{\alpha}F \tag{2}$$

where E_{pc} and $E_{pc/2}$ are the cathodic peak potential and half-peak potential, respectively. According to Eq. (2) and the data obtained from **Figure 2(a)**, the average transfer coefficient can be calculated as 0.53. Substituting this and other parameters in Eq. (1), the diffusion coefficient of Zn(II) in ChCl/urea-based DES is determined to be 6.21×10^{-9} cm^2 s^{-1} at 333 K, which is smaller than that of Zn(II) in Bu_3MeN-TFSI (1.6×10^{-7} cm^2 s^{-1} [54]) and $AlCl_3$-EMIC (2.6×10^{-6} cm^2 s^{-1} [55]) ionic liquids. The relatively low mobility of Zn(II) species may be ascribed to the formation of large, sterically hindered Zn-complex anions when ZnO is dissolved in the DES [44] and high viscosity of the ChCl/urea-based DES [56].

2.2. Morphology and phase composition analyses of the electrodeposited Zn films

The SEM images of the Zn films electrodeposited at different electrodeposition temperatures are shown in **Figure 3**. It is obvious that the microstructure of the Zn films changes gradually with increasing the electrodeposition temperature. As illustrated in **Figure 3(a)**, compact Zn films with particle size approximately 400 nm can be obtained at 333 K. The particle size of the Zn electrodeposits apparently increases with increasing electrodeposition temperature (**Figure 3b–d**). In addition, the interspaces between the Zn particles

http://dx.doi.org/10.5772/65883

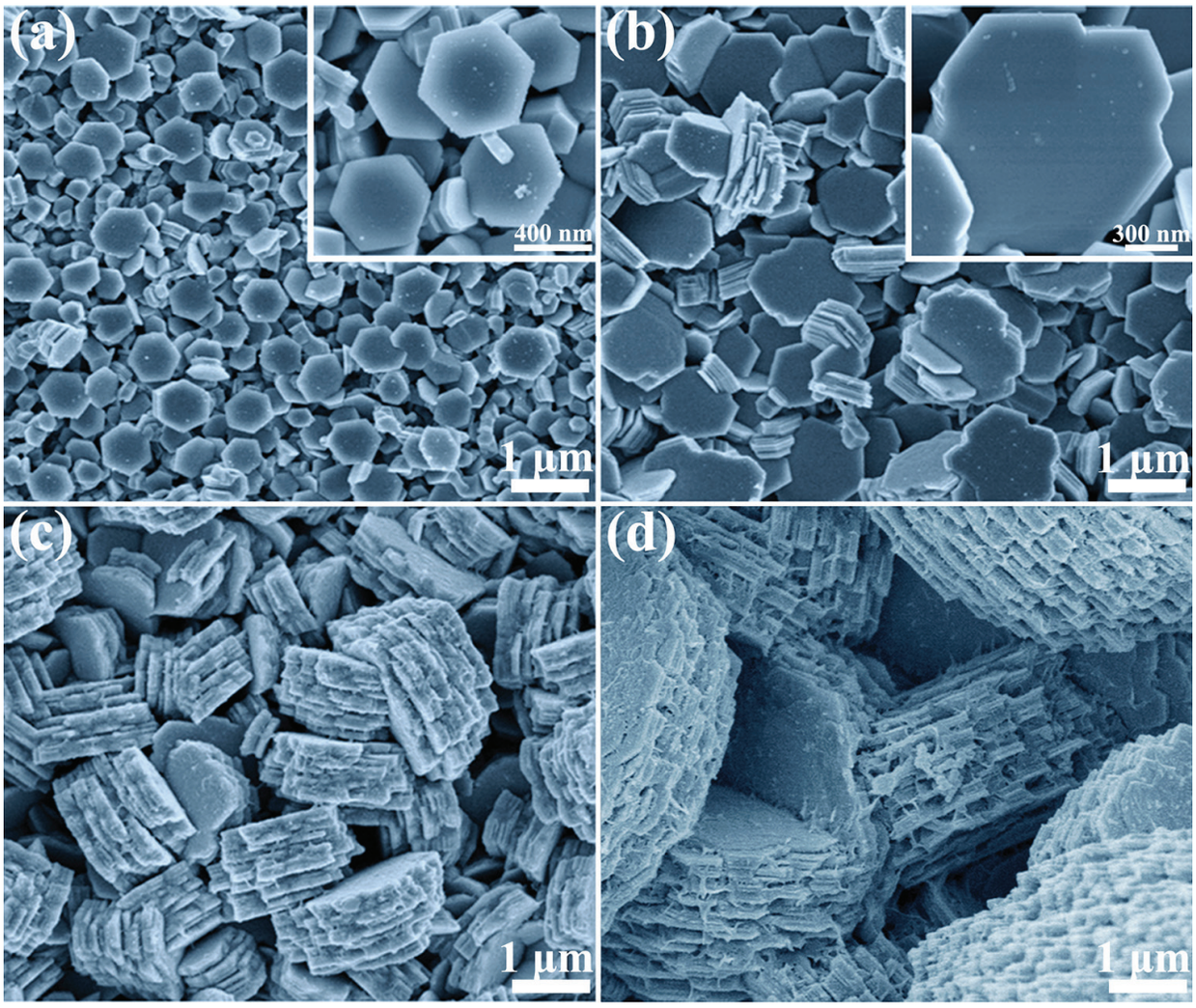

Figure 3. SEM images of the Zn electrodeposits obtained from ChCl/urea–ZnO (0.1 M) at –1.15 V on a Cu substrate at different temperatures: (a) 333 K, (b) 343 K, (c) 353 K, and (d) 363 K for 2 h.

also increase gradually with the growth of the particles, which result in the Zn films become porous. The Zn electrodeposits with hexagonal structure (**Figure 3a**) continue to further nucleate and grow to form polygonal Zn plates (**Figure 3b**) and then transform to multilayer structure (**Figure 3c–d**). The Zn particles gradually change from dispersive nanoparticle to multilayer microparticle with irregular shapes. It should be noted that the morphology change during the electrodeposition process is mainly attributed to the increased electrodeposition rate and the electrodeposition temperature. It is worth noting that the morphology of the electrodeposited Zn can be influenced by the electrodeposition temperature.

X-ray diffraction (XRD) pattern of the Zn electrodeposits on a Cu substrate obtained from 0. 1 M ZnO in ChCl/urea-based DES is shown in **Figure 4**. It can be seen that only two metallic phases, Zn and Cu (substrate), are identified. It is obvious that the electrodeposit is composed of high purity Zn.

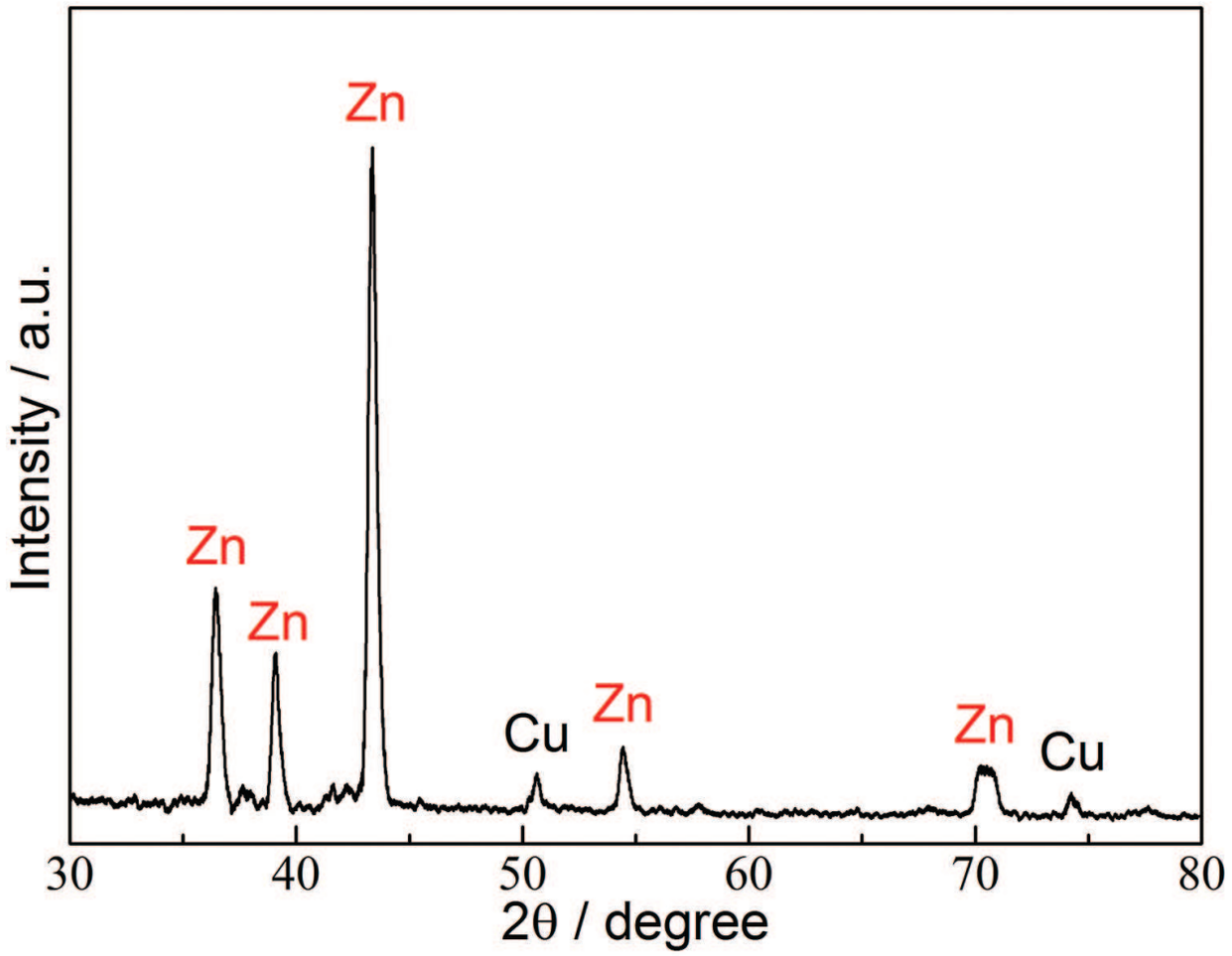

Figure 4. XRD pattern of the Zn electrodeposits obtained from ChCl/urea–ZnO (0.1 M) on a Cu substrate at –1.15 V and 333 K.

3. Electrodeposition of Cu from CuO in ChCl/EG and ChCl/urea-based DESs

3.1. CV study

In order to investigate the electrochemical behavior of Cu, CV analysis was carried out in ChCl/EG–CuO (0.01 M)- and ChCl/urea–CuO (0.01 M)-based DESs, and the CV curves are shown in **Figure 5**. For comparison, **Figure 5(a)** and **(b)** illustrates the voltammetric behavior of Cu(II) in the ChCl/EG–CuO (0.01 M) and ChCl/urea–CuO (0.01 M) electrolytes, respectively, and the CVs were recorded at 353 K with a scan rate of 10 mV s^{-1}. Two redox couples (c_1/a_1 and c_2/a_2) are occurred in each CV curve. The redox couple (c_1/a_1) is assigned to the reaction of Cu(II) + $e^- \leftrightarrow$ Cu(I), and the redox couple (c_2/a_2) is attributed to the reaction of Cu(I) + $e^- \leftrightarrow$ Cu. As shown in **Figure 5(a)** and **(b)**, the peak current density for the reduction of Cu(I)/Cu(0) in the ChCl/EG system is higher than that in the ChCl/urea system. Moreover, the redox potentials of the Cu(II)/Cu(I) and Cu(I)/Cu(0) couples in the ChCl/urea system occur at potentials more negative than those observed in the ChCl/EG system. The different redox potentials

http://dx.doi.org/10.5772/65883

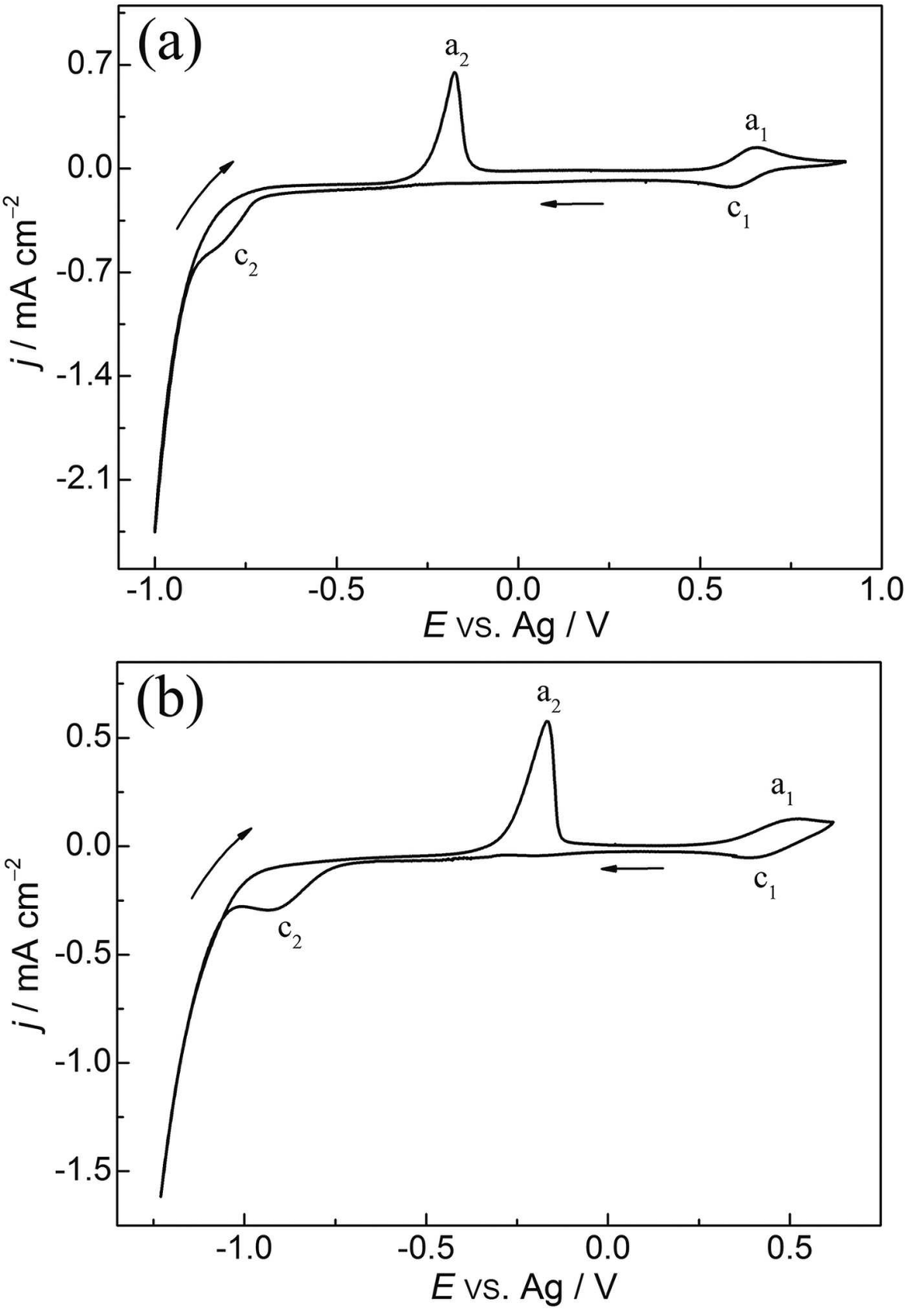

Figure 5. CV curves of a Fe electrode in (a) ChCl/EG–CuO (0.01 M) and (b) ChCl/urea–CuO (0.01 M) at 353 K with a scan rate of 10 mV s^{-1}.

may be attributed to the differences in ligand activity between the two DESs. There is a strong coordination between the chloride ions and urea, which can effectively decrease the activity of chloride compared with EG [25]. These results can be ascribed to the lower viscosity of the ChCl/EG system and the facile charge-transfer kinetics in the ChCl/EG system compared to that of the ChCl/urea system [41]. Therefore, the lower coordinated Cu species in the ChCl/EG ionic liquid are obviously more easier to be reduced, whereas the higher coordinated Cu species in the ChCl/urea ionic liquid are more difficult to be reduced.

3.2. Characterization of the Cu electrodeposits

The SEM images of the Cu films electrodeposited in ChCl/EG ionic liquid at different electrodeposition potentials are shown in **Figure 6**. In **Figure 6(a)**, a porous and nonuniform electrodeposit is formed. As the electrodeposition potential was made progressively negative to –0.80 V, the agglomeration of Cu particles occurred. The Cu particles generated at high cathodic potential are composed of some larger agglomerates with fine nanoscale particles (**Figure 6c**). **Figure 6(d)** shows the EDS spectra of the Cu film corresponding to **Figure 6(b)**. Only two elements Cu and Fe (substrate) are determined from the EDS spectra.

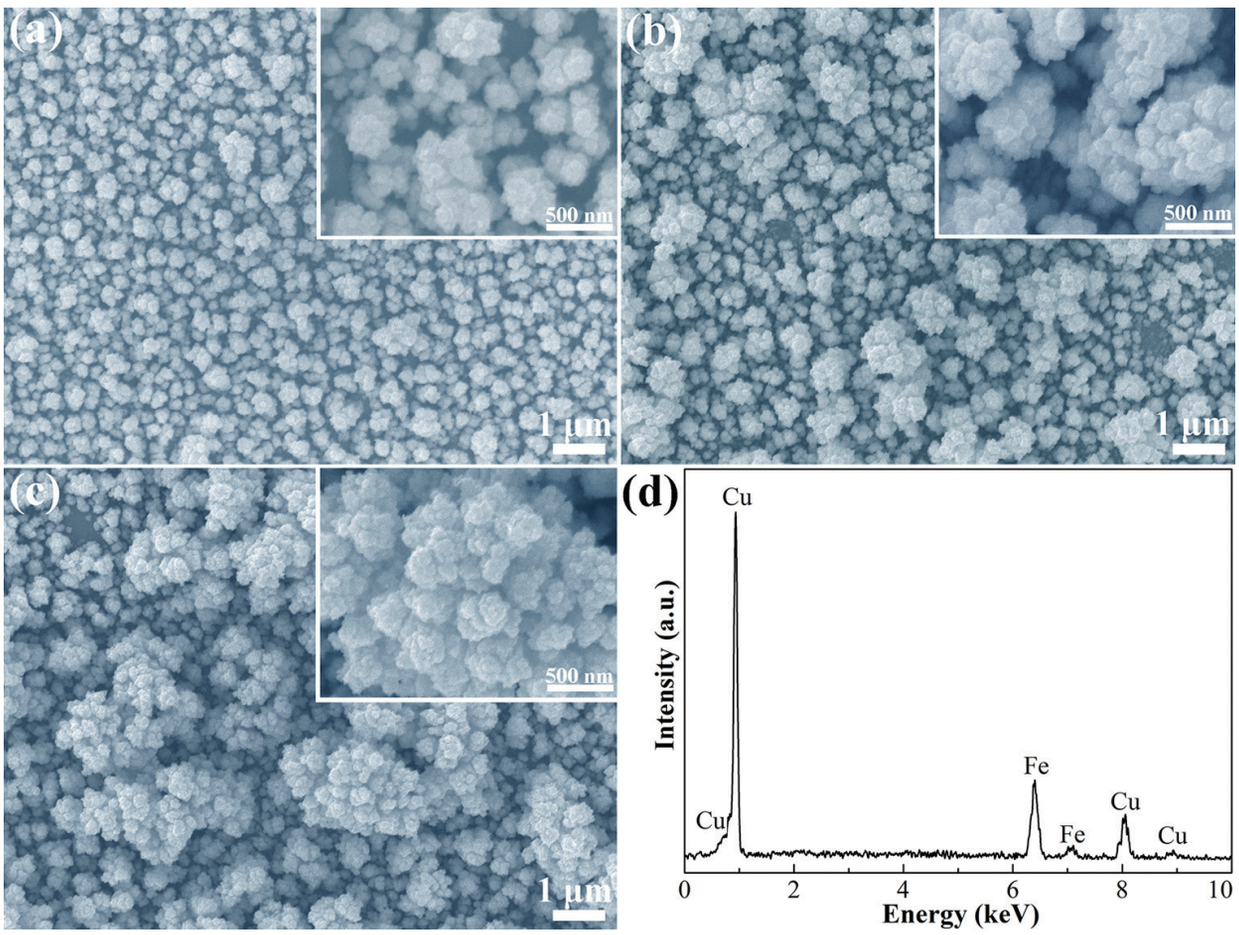

Figure 6. SEM images of the Cu electrodeposits obtained on a Fe substrate in ChCl/EG–CuO (0.01 M) at (a) –0.75 V, (b) –0.80 V, and (c) –0.85 V and 353 K for 3 h, and (d) EDS spectra of the electrodeposited Cu film corresponding to (b).

http://dx.doi.org/10.5772/65883

It is indicated that the electrodeposition potential has significant influences on the morphology of Cu electrodeposits.

The SEM images of the Cu films electrodeposited in ChCl/urea ionic liquid at different electrodeposition potentials are shown in **Figure 7**. As evidenced in **Figure 7(a)**, the uniform, dense, and compact electrodeposits are formed at −0.90 V. As the electrodeposition potential increases to –0.95 and –1.00 V, some spherical nodular electrodeposits are formed and become more porous (**Figure 7b** and **c**). **Figure 7(d)** shows the EDS spectra of the Cu film corresponding to **Figure 7(b)**. Only two elements Cu and Fe (substrate) are determined from the EDS spectra. The differences in morphology are probably due to the different Cu species formed in the electrolyte, the higher coordinated and lower superficial diffusion of Cu species in ChCl/urea ionic liquid results in a homogenous distribution of particles with particle size smaller than those observed in ChCl/EG ionic liquid.

XRD patterns of the Cu electrodeposits on a Fe substrate obtained from 0.01 M CuO in ChCl/EG and ChCl/urea ionic liquids are shown in **Figure 8(a)** and **(b)**. It can be seen that only two metallic phases Cu and Fe (substrate) are identified in both media. It is evidenced that the electrodeposit is composed of high purity Cu.

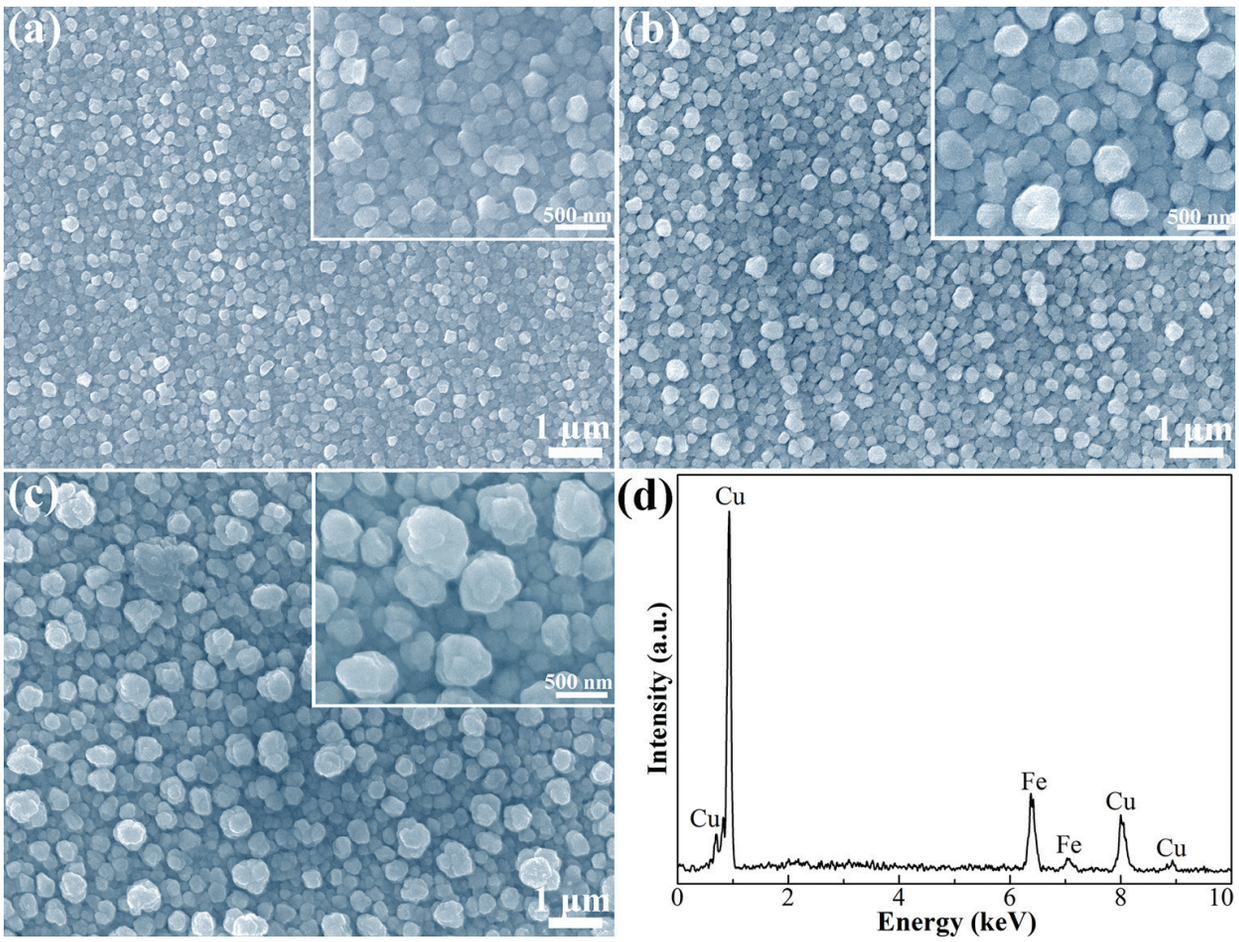

Figure 7. SEM images of the Cu electrodeposits obtained on a Fe substrate in ChCl/urea–CuO (0.01 M) at (a) –0.90 V, (b) –0.95 V, (c) –1.00 V and 353 K for 3 h, and (d) EDS spectra of the electrodeposited Cu film corresponding to (b).

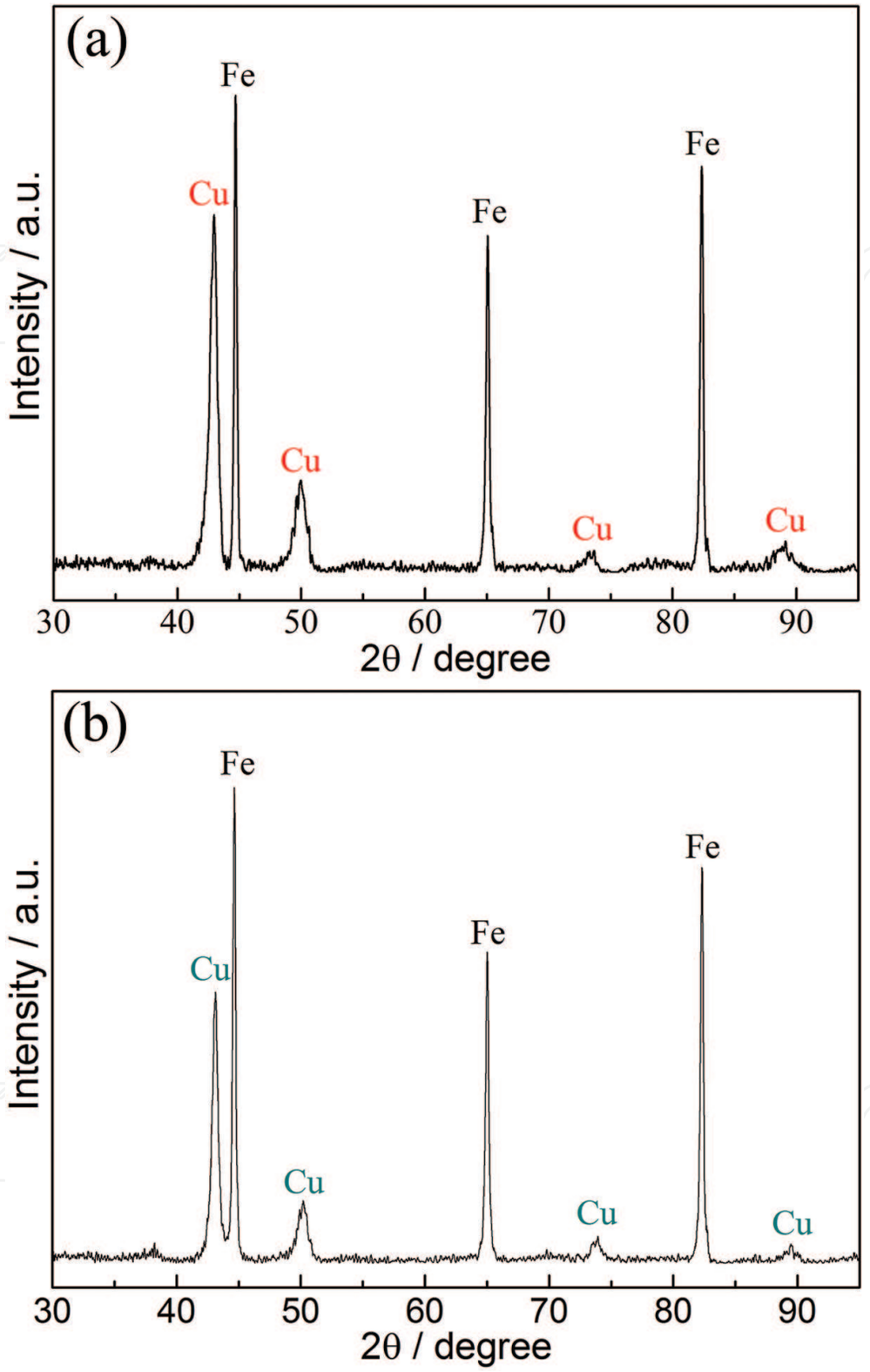

Figure 8. XRD patterns of the Cu electrodeposits obtained on a Fe substrate in (a) ChCl/EG–CuO (0.01 M) at –0.80 V and 353 K for 3 h and (b) ChCl/urea–CuO (0.01 M) at –0.95 V and 353 K for 3 h.

http://dx.doi.org/10.5772/65883

4. Electrodeposition of Zn-Cu alloys in ChCl/urea-based DES

4.1. CV analysis

Figure 9 shows the CV curve of the ChCl/urea ionic liquid dissolved with 0.01 M CuO and 0.1 M ZnO on a Fe electrode at 343 K with a scan rate of 10 mV s^{-1}. There are three reduction peaks on the cathodic branch of the voltammogram. The two cathodic reduction peaks observed at approximately 0.25 V (labeled as c_1) and –0.85 V (c_2) are attributed to the Cu(II) to Cu(I) reduction process and the Cu(I) to Cu reduction process, respectively. The reduction peak at about –1.15 V (c_3) can be ascribed to the Zn(II) to Zn reduction process. When the scan is reversed, four oxidation peaks (a_1, a_2, a_3, and a_4), as shown in **Figure 9**, are observed in the potential range of –1.10 to 0.50 V. The oxidation peaks for pure Cu (a_1 and a_2) and pure Zn (a_4) are at about 0.32, –0.30, and –1.05 V, respectively, and the oxidation peak (a_3) is for the Zn-Cu electrodeposits between the two potentials (a_2 and a_4).

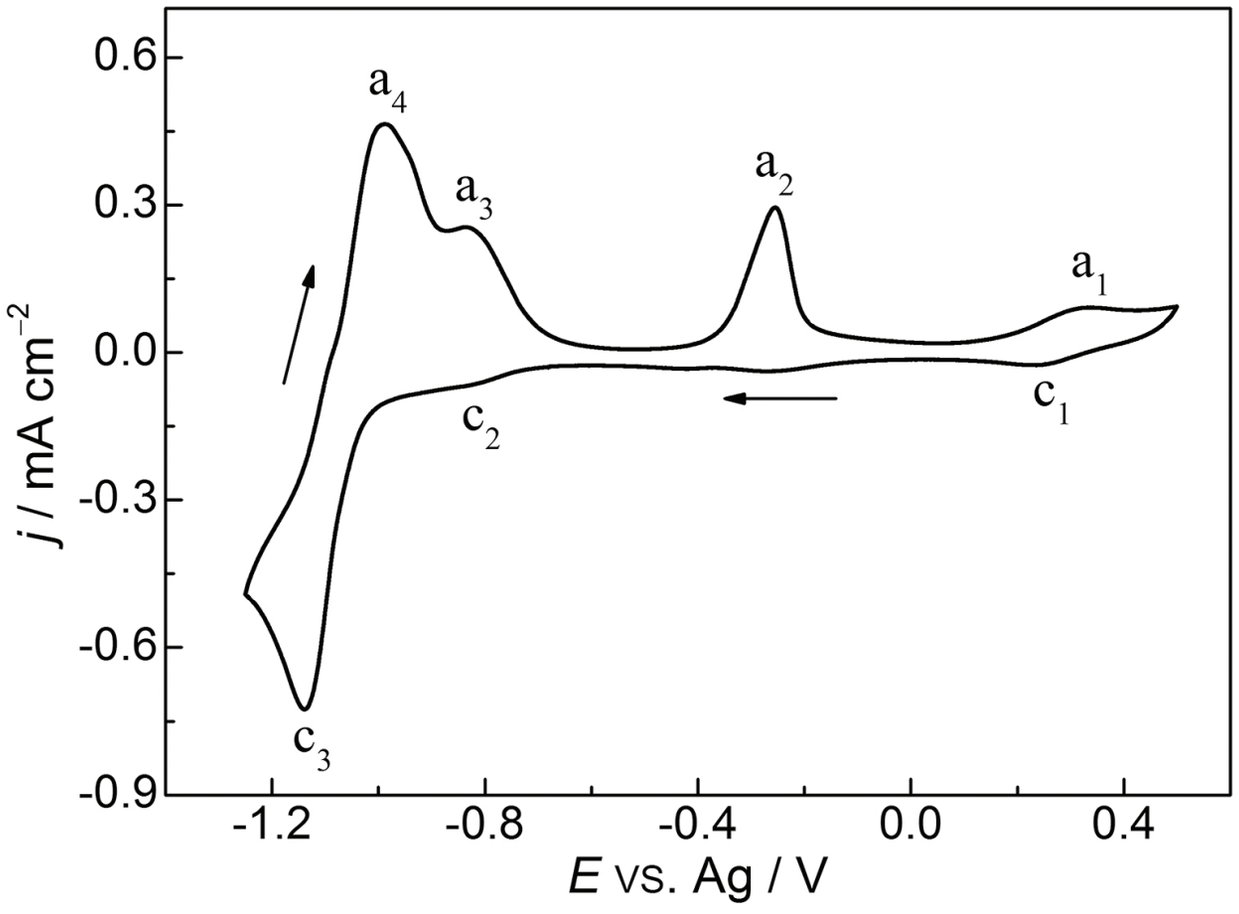

Figure 9. CV curve of a Fe electrode in ChCl/urea ionic liquid containing 0.1 M ZnO and 0.01 M CuO at 343 K with a scan rate of 10 mV s^{-1}.

4.2. Morphology and phase composition analyses of the electrodeposited Zn-Cu films

The XRD patterns of the Zn-Cu alloys electrodeposited on a Fe substrate in the ChCl/urea ionic liquid containing 0.1 M ZnO and 0.01 M CuO at different potentials and 343 K for 3 h are shown in **Figure 10(a)**. It can be seen that the dominate phases of the Zn-Cu films electrodeposited at –1.05 V are Cu_5Zn_8 and Cu (substrate). As the electrodeposition potential increases to –1.10 V, two new phases ($CuZn_5$, Zn) are observed and the Cu_5Zn_8 phase is disappeared. It is mainly the result of increasing the Zn electrodeposition rate under more negative potential. **Figure 10(b)** and **(c)** shows the SEM images of the Zn-Cu alloys electrodeposited in the ChCl/urea ionic liquid containing 0.1 M ZnO and 0.01 M CuO at different cathodic potentials and 343 K for 3 h. The Zn-Cu electrodeposit obtained at –1.05 V is composed of spherical clusters with some void space between the particles (**Figure 10b**). When the potential changes from –1.05 to –1.10 V, the agglomeration of Zn-Cu particles is observed and the electrodeposits are porous and nonuniform (**Figure 10c**).

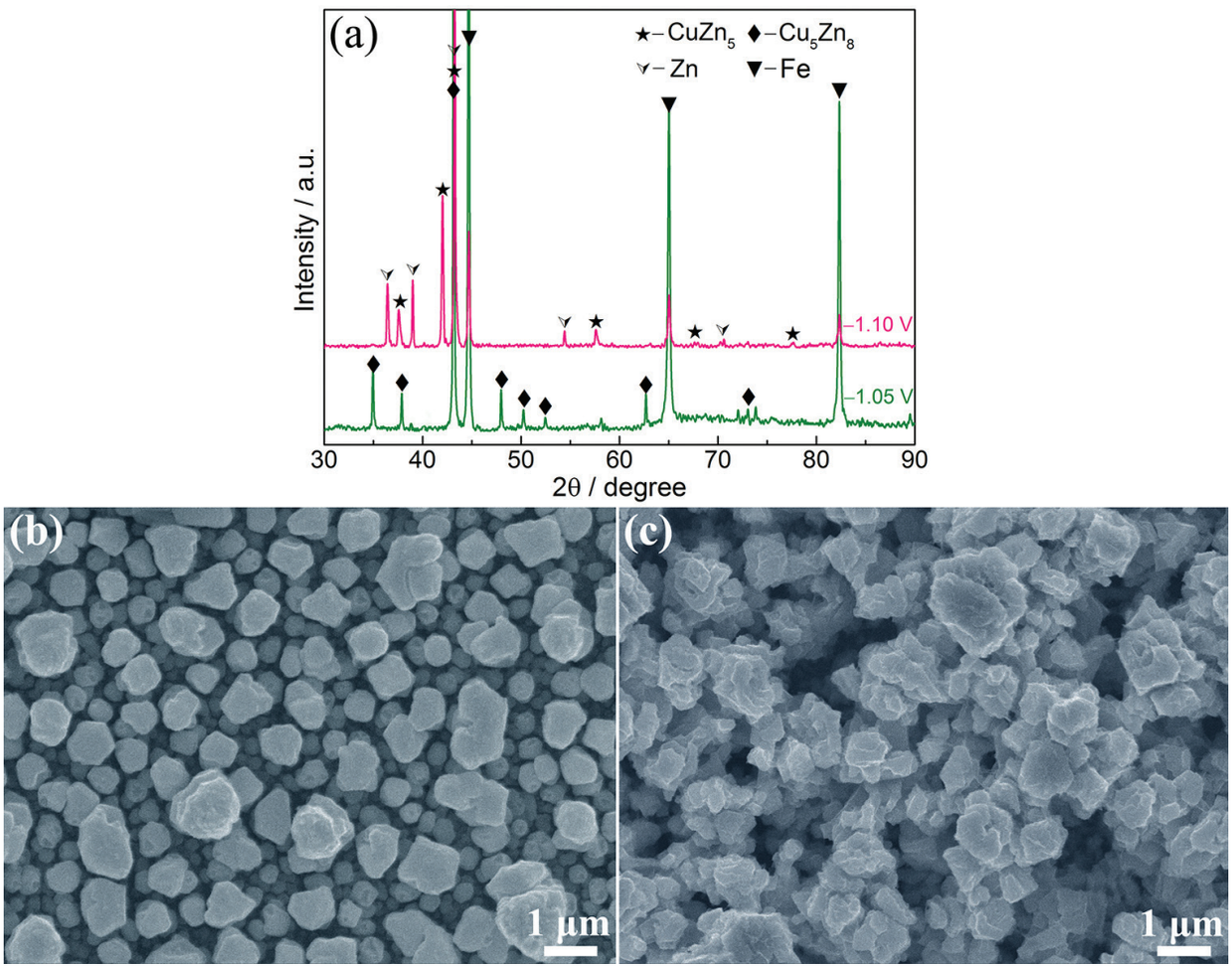

Figure 10. (a) XRD patterns of the Cu–Zn alloys electrodeposited on a Fe substrate in the ChCl/urea ionic liquid containing 0.1 M ZnO and 0.01 M CuO at different cathodic potentials and 343 K for 3 h. (b) and (c) SEM images of the Cu–Zn electrodeposits obtained on a Fe substrate in the 12CU ionic liquid containing 0.1 M ZnO and 0.01 M CuO at 343 K for 3 h, (b) –1.05 V and (c) –1.10 V.

5. Conclusions

The electrodeposition of Zn, Cu, and Zn-Cu alloys from ZnO/CuO precursors has been investigated in DESs. Electrochemical measurements showed that the Zn electrodeposition is a diffusion-controlled quasi-reversible, one-step, two electrons transfer process. The diffusion coefficient of Zn(II) was estimated to be 6.21×10^{-9} cm^2 s^{-1} at 333 K. Uniform, dense, and compact Zn electrodeposits can form under suitable electrodeposition potentials and lower temperatures. Besides, the electrodeposition of Cu from CuO in the eutectics based on ChCl with urea and EG has been respectively investigated and compared. The voltammetric measurements show the electrodeposition of Cu in ChCl/EG and ChCl/urea systems through a two-step process. The higher coordinated Cu species in the ChCl/urea ionic liquid are more difficult to be reduced. The surface morphology of the Cu electrodeposits can be significantly affected by the ionic liquids and the electrodeposition potential. Furthermore, the Cu electrodeposits obtained in the ChCl/urea ionic liquid possess more homogenous microstructures than those produced in the ChCl/EG ionic liquid. In addition, the Zn-Cu alloy films have also been electrodeposited directly from their metal oxide precursors in ChCl/urea-based DES, the phase composition of the Zn-Cu alloys depends on the electrodeposition potential. These results may have implications on the electrodeposition of other alloy films from oxide precursors in DESs system.

Acknowledgements

The authors thank China National Funds for Distinguished Young Scientists (No. 51225401), the National Natural Science Foundation of China (Nos. 51304132 and 51574164), the National Basic Research Program of China (No. 2014CB643403), the Science and Technology Commissions of Shanghai Municipality (No. 14JC1491400), and the Young Teacher Training Program of Shanghai Municipal Education Commission for financial support. The authors also thank the Instrumental Analysis and Research Center of Shanghai University for materials characterization.

Author details

Xingli Zou*, Xionggang Lu* and Xueliang Xie

*Address all correspondence to: xlzou@shu.edu.cn and luxg@shu.edu.cn

State Key Laboratory of Advanced Special Steel & Shanghai Key Laboratory of Advanced Ferrometallurgy & School of Materials Science and Engineering, Shanghai University, Shanghai, China

References

[1] Liu H, Szunerits S, Xu WX. Preparation of superhydrophobic coatings on zinc as effective corrosion barriers. ACS Appl. Mat. Interfaces. 2009;**1**:1150–1153. DOI: 10.1021/am900100q

[2] Liu Z, Zein El Abedin S, Endres F. Electrodeposition and stripping of zinc from an ionic liquid polymer gel electrolyte for rechargeable zinc-based batteries. J. Solid State Electrochem. 2014;**18**:2683–2691. DOI: 10.1007/s10008-014-2526-8

[3] Fashu S, Gu C, Wang XX. Influence of electrodeposition conditions on the microstructure and corrosion resistance of Zn-Ni alloy coatings from a deep eutectic solvent. Surf. Coat. Technol. 2014;**242**:34–41. DOI: 10.1016/j.surfcoat.2014.01.014

[4] Abbott A, Frisch G, Ryder K. Electroplating using ionic liquids. Annu. Rev. Mater. Res. 2013;**43**:335–358. DOI: 10.1146/annurev-matsci-071312-121640

[5] Peterson A, Abild-Pedersen F, Studt FX. How copper catalyzes the electroreduction of carbon dioxide into hydrocarbon fuels. Energy Environ. Sci. 2010;**3**:1311–1315. DOI: 10.1039/c0ee00071j

[6] Ding Y, Chen M, Erlebacher J. Metallic mesoporous nanocomposites for electrocatalysis. J. Am. Chem. Soc. 2004;**126**:6876–6877. DOI: 10.1021/ja0320119

[7] Miura S, Honma H. Advanced copper electroplating for application of electronics. Surf. Coat. Technol. 2003;**169-170**:91–95. DOI: 10.1016/S0257-8972(03)00165-8

[8] Brown A, Melsenhelder J, Yao N. The alkaline electrolytic process for zinc production: a critical evaluation. Ind. Eng. Chem. Prod. Res. Dev. 1983;**22**:263–272. DOI: 10.1021/i300010a020

[9] Guillaume P, Leclerc N, Boulanger CX. Investigation of optimal conditions for zinc electrowinning from aqueous sulfuric acid electrolytes. J. Appl. Electrochem. 2007;**37**:1237–1243. DOI: 10.1007/s10800-007-9377-2

[10] Yan H, Downes J, Boden PX. A model for nanolaminated growth patterns in Zn and Zn-Co electrodeposits. J. Electrochem. Soc. 1996;**143**:1577–1583. DOI: 10.1149/1.1836682

[11] Gomes A, da Silva Pereira M. Pulsed electrodeposition of Zn in the presence of surfactants. Electrochim. Acta 2006;**51**:1342–1350. DOI: 10.1016/j.electacta.2005.06.023

[12] Mackinnon D, Brannen J, Kerby R. The effect of lead on zinc deposit structures obtained from high purity synthetic and industrial acid sulphate electrolytes. J. Appl. Electrochem. 1979;**9**:55–70. DOI: 10.1007/BF00620587

[13] Nikolić N, Popov K, Pavlović LjX. The effect of hydrogen codeposition on the morphology of copper electrodeposits. I. The concept of effective overpotential. J. Electroanal. Chem. 2006;**588**:88–98. DOI: 10.1016/j.jelechem.2005.12.006

[14] Abdelkader A, Kilby K, Cox AX. DC voltammetry of electro-deoxidation of solid oxides. Chem. Rev. 2013;**113**:2863–2886. DOI: 10.1021/cr200305x

[15] Zou X, Lu X, Zhou ZX. Electrochemical extraction of Ti_5Si_3 silicide from multicomponent Ti/Si-containing metal oxide compounds in molten salt. J. Mater. Chem. A 2014;**2**:7421–7430. DOI: 10.1039/c3ta15039a

[16] Zou X, Gu S, Cheng HX. Facile electrodeposition of iron films from $NaFeO_2$ and Fe_2O_3 in alkaline solutions. J. Electrochem. Soc. 2015;**162**:D49–D55. DOI: 10.1149/2.0751501jes

[17] Endres F, Abbott A, MacFarlane D (Eds.). Electrodeposition from Ionic Liquids. Wiley-VCH, Weinheim, 2008.

[18] Castner Jr E, Wishart J. Spotlight on ionic liquids. J. Chem. Phys. 2010;**132**:120901–120909. DOI: 10.1063/1.3373178

[19] Hartley J, Ip C, Forrest GX. EXAFS Study into the speciation of metal salts dissolved in ionic liquids and deep eutectic solvents. Inorg. Chem. 2014;**53**:6280–6288. DOI: 10.1021/ic500824r

[20] Dogel J, Freyland W. Layer-by-layer growth of zinc during electrodeposition on Au(111) from a room temperature molten salt. Phys. Chem. Chem. Phys. 2003;**5**:2484–2487. DOI: 10.1039/b303388k

[21] Hsiu S, Huang J, Sun IX. Lewis acidity dependency of the electrochemical window of zinc chloride–1-ethyl-3-methylimadazolium chloride ionic liquids. Electrochim. Acta 2002;**47**;4367–4372. DOI: 10.1016/S0013-4686(02)00509-1

[22] Abbott A, Barron J, Ryder K. Electrolytic deposition of Zn coatings from ionic liquids based on choline chloride. Trans. Inst. Met. Finish. 2009;**87**:201–207. DOI: 10.1179/174591909X438857

[23] Whitehead A, Pölzler M, Gollas B. Zinc electrodeposition from a deep eutectic system containing choline chloride and ethylene glycol. J. Electrochem. Soc. 2010;**157**:D328–D334. DOI: 10.1149/1.3364930

[24] Abbott A, Barron J, Frisch GX. Double layer effects on metal nucleation in deep eutectic solvents. Phys. Chem. Chem. Phys. 2011;**13**:10224–10231. DOI: 10.1039/C0CP02244F

[25] Abbott A, Barron J, Frisch GX. The effect of additives on zinc electrodeposition from deep eutectic solvents. Electrochim. Acta 2011;**56**:5272–5279. DOI: 10.1016/j.electacta.2011.02.095

[26] Pereira N, Fernandes P, Pereira CX. Electrodeposition of zinc from choline chloride-ethylene glycol deep eutectic solvent: effect of the tartrate ion. J. Electrochem. Soc. 2012;**159**:D501–D506. DOI: 10.1149/2.004209jes

[27] Liu Z, Abedin S, Endres F. Electrodeposition of zinc films from ionic liquids and ionic liquid/water mixtures. Electrochim. Acta 2013;**89**:635–643. DOI: 10.1016/j.electacta.2012.11.077

[28] Zheng Y, Dong K, Wang QX. Electrodeposition of zinc coatings from the solutions of zinc oxide in imidazolium chloride/urea mixtures. Sci. China: Chem. 2012;**55**:1587–1597. DOI: 10.1007/s11426-012-4682-y

[29] Endres F. Ionic liquids: Solvents for the electrodeposition of metals and semiconductors. Chemphyschem. 2002;**3**:144–154. DOI: 10.1002/1439-7641

[30] Endres F, Schweizer A. The electrodeposition of copper on Au(111) and on HOPG from the 66/34 mol% aluminium chloride/1-butyl-3-methylimidazolium chloride room temperature molten salt: an EC-STM study. Phys. Chem. Chem. Phys. 2000;**2**:5455–5462. DOI: 10.1039/B006040M

[31] Chen P, Sun I. Electrochemical study of copper in a basic 1-ethyl-3-methylimidazolium tetrafluoroborate room temperature molten salt. Electrochim. Acta 1999;**45**:441–450. DOI: 10.1016/S0013-4686(99)00275-3

[32] Murase K, Nitta K, Hirato TX. Electrochemical behaviour of copper in trimethyl-n-hexylammonium bis((trifluoromethyl)sulfonyl)amide, an ammonium imide-type room temperature molten salt. J. Appl. Electrochem. 2001;**31**:089–1094. DOI: 10.1023/A:1012255601793

[33] Zein El Abedin S, Saad A, Farag HX. Electrodeposition of selenium, indium and copper in an air- and water-stable ionic liquid at variable temperatures. Electrochim. Acta 2007;**52**:2746–2754. DOI: 10.1016/j.electacta.2006.08.064

[34] Chen P, Deng M, Zhuang D. Electrochemical codeposition of copper and manganese from room-temperature N-butyl-N-methylpyrrolidinium bis(trifluoromethylsulfonyl)imide ionic liquid. Electrochim. Acta 2009;**54**:6935–6940. DOI: 10.1016/j.electacta.2009.07.016

[35] Endres F, Zein El Abedin S. Air and water stable ionic liquids in physical chemistry. Phys. Chem. Chem. Phys. 2006;**8**:2101–2116. DOI: 10.1039/B600519P

[36] Haerens K, Matthijs E, Binnemans KX. Electrochemical decomposition of choline chloride based ionic liquid analogues. Green Chem. 2009;**11**:1357–1365. DOI: 10.1039/B906318H

[37] Chen P, Chang Y. Voltammetric study and electrodeposition of copper in 1-butyl-3-methylimidazolium salicylate ionic liquid. Electrochim. Acta 2012;**75**:339–346. DOI: 10.1016/j.electacta.2012.05.024

[38] Abbott A, Capper G, Davies DX. Novel solvent properties of choline chloride/urea mixtures. Chem. Commun. 2003:70–71. DOI: 10.1039/B210714G

[39] Abbott A, Boothby D, Capper GX. Deep eutectic solvents formed between choline chloride and carboxylic acids: versatile alternatives to ionic liquids. J. Am. Chem. Soc. 2004;**126**:9142–9147. DOI: 10.1021/ja048266j

[40] Abbott A, Ttaib K, Frisch GX. Electrodeposition of copper composites from deep eutectic solvents based on choline chloride. Phys. Chem. Chem. Phys. 2009;**11**:4269–4277. DOI: 10.1039/B817881J

[41] Yang H, Reddy R. Electrochemical deposition of zinc from zinc oxide in 2:1 urea/choline chloride ionic liquid. Electrochim. Acta 2014;**147**:513–519. DOI: 10.1016/j.electacta.2014.09.137

[42] Yang H, Reddy R. Fundamental studies on electrochemical deposition of lead from lead oxide in 2:1 urea/choline chloride ionic liquids. J. Electrochem. Soc. 2014;**161**:D586–D592. DOI: 10.1149/2.1161410jes

[43] Tsuda T, Boyd L, Kuwabata SX. Electrochemistry of copper(I) oxide in the 66.7–33.3 mol % urea–choline chloride room-temperature eutectic melt. J. Electrochem. Soc. 2010;**157**:F96–F103. DOI: 10.1149/1.3377117

[44] Xie X, Zou X, Lu XX. Electrodeposition of Zn and Cu–Zn alloy from ZnO/CuO precursors in deep eutectic solvent. Appl. Surf. Sci. 2016;**385**:481–489. DOI: 10.1016/j.apsusc.2016.05.138.

[45] Xie X, Zou X, Lu XX. Voltammetric study and electrodeposition of Cu from CuO in deep eutectic solvents. J. Electrochem. Soc. 2016; **163**:D537–D543.DOI:10.1149/2.1241609jes.

[46] Zhang Q, Abbott A, Yang C. Electrochemical fabrication of nanoporous copper films in choline chloride-urea deep eutectic solvent. Phys. Chem. Chem. Phys. 2015;**17**:14702–14709. DOI: 10.1039/c5cp01276g

[47] Ru J, Hua Y, Wang DX. Mechanistic insight of in situ electrochemical reduction of solid PbO to lead in ChCl-EG deep eutectic solvent. Electrochim. Acta 2015;**186**:455–464. DOI: 0.1016/j.electacta.2015.11.013

[48] Abbott A, Capper G, Davies DX. Selective extraction of metals from mixed oxide matrixes using choline-based ionic liquids. Inorg. Chem. 2005;**44**:6497–6499. DOI: 10.1021/ic0505450

[49] Abbott A, Capper G, Davies DX. Solubility of metal oxides in deep eutectic solvents based on choline chloride. J. Chem. Eng. Data 2006;**51**:1280–1282. DOI: 10.1021/je060038c

[50] Abbott A, Collins J, Dalrymple IX. Processing of electric arc furnace dust using deep eutectic solvents. Aust. J. Chem. 2009;**62**:341–347. DOI: 10.1071/CH08476

[51] Bard A, Faulkner L. Electrochemical methods: Fundamentals and Applications. John Wiley & Sons, New York, 2000.

[52] Nagaishi R, Arisaka M, Kimura TX. Spectroscopic and electrochemical properties of europium (III) ion in hydrophobic ionic liquids under controlled condition of water content. J. Alloys Compd. 2007;**431**:221–225. DOI: 10.1016/j.jallcom.2006.05.048

[53] Kuznetsov S, Gaune-Escard M. Kinetics of electrode processes and thermodynamic properties of europium chlorides dissolved in alkali chloride melts. J. Electroanal. Chem. 2006;**595**:11–22. DOI: 10.1016/j.jelechem.2006.02.036

[54] Chen P, Hussey C. The electrodeposition of Mn and Zn-Mn alloys from the room-temperature tri-1-butylmethylammonium bis((trifluoromethane)sulfonyl)imide ionic liquid. Electrochim. Acta 2007;**52**:1857–1864. DOI: 10.1016/j.electacta.2006.07.049

[55] Pitner W, Hussey C. Electrodeposition of zinc from the Lewis acidic aluminum chloride-1-methyl-3-ethylimidazolium chloride room temperature molten salt. J. Electrochem. Soc. 1997;**144**:3095–3103. DOI: 10.1149/1.1837965

[56] Abbott A, Azam M, Frisch GX. Ligand exchange in ionic systems and its effect on silver nucleation and growth. Physical Chemistry Chemical Physics. 2013;**15**:17314–17323. DOI: 10.1039/c3cp52674g

IntechOpen